Development of an Antimicrobial Peptide SAAP-148-Functionalized Supramolecular Coating on Titanium to Prevent Biomaterial-Associated Infections

ADVANCED MATERIALS TECHNOLOGIES
www.advmattechnol.de

Development of an Antimicrobial Peptide SAAP-148-Functionalized Supramolecular Coating on Titanium to Prevent Biomaterial-Associated Infections

Moniek G. J. Schmitz, Martijn Riool, Leonie de Boer, Annika F. Vrehen, Paul A. A. Bartels, Sebastian A. J. Zaat, and Patricia Y. W. Dankers**

Titanium implants are widely used in medicine but have a risk of biomaterial-associated infection (BAI), of which traditional antibiotic-based treatment is affected by resistance. Antimicrobial peptides (AMPs) are used to successfully kill antibiotic-resistant bacteria. Herein, a supramolecular coating for titanium implants is developed which presents the synthetic antimicrobial and antibiofilm peptide SAAP-148 via supramolecular interactions using ureido-pyrimidinone supramolecular units (UPy-SAAP-148GG). Material characterization of dropcast coatings shows the presence of UPy-SAAP-148GG at the surface. The supramolecular immobilized peptide remains antimicrobially active in dropcast polymer films and can successfully kill (antibiotic-resistant) *Staphylococcus aureus*, *Acinetobacter baumannii*, and *Escherichia coli*. Minor toxicity for human dermal fibroblasts is observed, with a reduced cell attachment after 24 h. Subsequently, a dipcoat coating on titanium implants is developed and tested in vivo in a subcutaneous implant infection mouse model with *S. aureus* administered locally on the implant before implantation to mimic contamination during surgery. The supramolecular coating containing 5 mol% of UPy-SAAP-148GG significantly prevents colonization of the implant surface as well as of the surrounding tissue, with no signs of toxicity. This shows that supramolecular AMP coatings on titanium are eminently suitable to prevent BAI.

1. Introduction

Due to their excellent mechanical and chemical properties, good corrosion resistance, and biocompatibility, titanium and its alloys are widely used in the medical field.[1] Titanium is a biomaterial commonly used as implanted medical device, such as in bone fusion, bone fixation, and joint replacement surgery (arthroplasty),[1] for dental implants[2] and for the body of ventricular assist devices.[3] However, the presence of a biomaterial in host tissue strongly induces the susceptibility to infection,[4,5] one of the main causes of implant failure.[1] Despite tremendous advances in the quality of healthcare, the probability of infection during a surgical procedure is still high, as implants can be contaminated during surgery by bacteria originating from the skin of the patients[6] or from the surgical environment.[7] Planktonic bacteria adhere to the implant surface and ultimately form a biofilm,[8] an important aspect in the pathogenesis of

M. G. J. Schmitz, A. F. Vrehen, P. A. A. Bartels, P. Y. W. Dankers
Department of Biomedical Engineering
Laboratory of Chemical Biology
Institute for Complex Molecular Systems
Eindhoven University of Technology
PO Box 513, Eindhoven 5600 MB, The Netherlands
E-mail: p.y.w.dankers@tue.nl

M. Riool[+], L. de Boer, S. A. J. Zaat
Department of Medical Microbiology and Infection Prevention
Amsterdam institute for Infection and Immunity
Amsterdam UMC
University of Amsterdam
Meibergdreef 9, Amsterdam 1105 AZ, The Netherlands
E-mail: s.a.zaat@amsterdamumc.nl

The ORCID identification number(s) for the author(s) of this article can be found under https://doi.org/10.1002/admt.202201846

[+]Present address: Laboratory of Experimental Trauma Surgery, Department of Trauma Surgery, University Hospital Regensburg, Am Biopark 9, 93053 Regensburg, Germany

DOI: 10.1002/admt.202201846

biomaterial-associated infection (BAI). Another aspect is the survival of bacteria in the tissue surrounding the implant, due to local derangement of the immune response caused by the combined presence of bacteria and a biomaterial.[9] BAI is mostly caused by staphylococci, in particular *Staphylococcus aureus* and *Staphylococcus epidermidis*, and streptococci, Gram-negative bacilli, enterococci, and anaerobes.[10–12] Due to the ability of bacteria to reside in biofilms, in host tissue, or even to hide intracellularly and thereby being protected against the immune response and antibiotic treatment, bacteria have multiple escape routes which makes these BAIs extremely difficult to treat.[13] Therefore, it is critical to prevent these types of infections.

Clinically, BAIs are mainly prevented by the application of skin antiseptics prior to surgery, such as iodine povidone or chlorhexidine, and systemic antibiotic prophylaxis such as intravenous administration of cefazolin before the surgical procedure.[14] Although systemic antibiotic prophylaxis leads to reduced infection rates, local antibiotic prophylaxis has been shown to provide a higher antibiotic dose and bioavailability at the wound or bone site with minimal toxic effects.[15,16] However, due to the increasing antimicrobial resistance development, the number of options available for prophylaxis becomes extremely limited.

To prevent BAI, various strategies for rendering implants antimicrobial have been developed, including antifouling/nonadhesive, contact-killing, and antimicrobial-releasing coatings.[1,17,18] Multifunctional coatings, which are both contact-killing and releasing an antimicrobial agent, are most promising since immobilization of antimicrobials on the surface of an implant may prevent contamination during surgery and thereby inhibit biofilm formation and subsequent peri-implant tissue colonization, while additional released antimicrobials fight bacteria which immediately escape into the tissue after implantation.[19] Cationic antimicrobial peptides (AMPs) are considered promising candidates to fight BAI as they are active against a broad spectrum of (antimicrobial-resistant) planktonic bacteria and biofilms.[17,20–21] The mode mechanism of action of AMPs, i.e., destruction of the microbial membrane, is considered to be less likely to cause resistance development.[22] It is important that the structural characteristics required for the antimicrobial activity of the AMPs are not altered during immobilization. Moreover, length, flexibility, spacer and orientation of the peptide, and its surface density should be taken into account.[23]

Supramolecular chemistry allows for a modular approach to introduce desired chemical, physical, or biological properties into a material in a controlled way. Moreover, by varying the molecular design, surface functionalization as well as sustained release profiles can be designed. This makes it suited for the design of multifunctional materials which are contact-killing, releasing, and tissue integrating all at the same time. Besides this, different supramolecular polymers can be developed, which are easily processable and with a variety of mechanical and degradable properties. This all, in combination with the in nature reversible interactions of supramolecular materials, allow high dynamics and tunability which makes them suitable for biomaterial design.[24]

In our group, supramolecular biomaterials based on the ureido-pyrimidinone (UPy) motif have been developed, which self-dimerize upon fourfold hydrogen bonding.[25,26] Functionalization of UPy-moieties with additional urea groups connected via an alkyl-linker introduced hydrogen bonding in the lateral direction. Aided by π–π interactions between UPy-dimers, this additional hydrogen bonding resulted in the formation of supramolecular stacks that are bundled into hierarchical fibers.[27,28] The introduction of the UPy hydrogen bonding moiety in short prepolymers and/or oligomers[29] in either a telechelic,[30] chain-extended,[31] or grafted fashion,[32] results in the formation of thermoplastic elastomers with a variety of mechanical properties. These UPy-fibers can be functionalized with bioactive compounds via a modular mix-and-match approach in which the UPy-base polymer is mixed with a UPy-functionalized additive.[30] This supramolecular approach is very versatile and has already successfully been used to introduce antimicrobial properties as contact-killing surface into the base material in vitro.[33]

In this study, a telechelically UPy-functionalized polycaprolactone with an M_n of 2 kDa (i.e., PCLdiUPy) was used as the base polymer and mixed with a potent UPy-modified AMP. More specifically, the AMP was based on the human cathelicidin LL-37 (LLGDFFRKSKEKIGKEFKRIVQRIKDFL-RNLVPRTES). LL-37 has served as template for the design of many antimicrobial, antibiofilm, immune modulating, and anticancer peptides.[34] In the development of an AMP, P60.4Ac (IGKEFKRIVERIKR-FLRELVRPLR; based on the highlighted part in LL-37 sequence) was developed which later was called OP-145.[35] This peptide showed improved antimicrobial activity compared to LL-37, but suffered from reduced activity in biological fluids.[36] A new screen, with additional peptide variants, resulted in the identification of the novel synthetic antimicrobial and antibiofilm peptide SAAP-148. SAAP-148 already has proven to be effective in vitro against a wide range of antibiotic-resistant bacteria, against biofilms in vitro, and in vivo as a topical cream in a murine wound biofilm infection model.[37] In this study, SAAP-148 is modified with a UPy-moiety (UPy-SAAP-148GG) and mixed with PCLdiUPy to develop a supramolecular antimicrobial coating for titanium implants (**Figure 1**A) which is able to prevent BAI. This approach allows to coat various types and shapes of biomaterials, including geometrically complex-shaped titanium implants, using newly discovered antimicrobials like AMPs in an easy mix-and-match fashion.

First, a dropcast coating on glass was developed and the material properties, the bactericidal activity against (multidrug-resistant; MDR) *S. aureus*, *Acinetobacter baumannii*, and *Escherichia coli*, and the effect on the morphology and metabolic activity of human dermal fibroblasts are assessed. Subsequently, a dipcoat coating on titanium implants was developed and its efficacy is evaluated at 1 and 4 days after implantation, in a mouse subcutaneous implant infection model.[9,36] Here, the *S. aureus* bacteria are not injected along the implants but administered directly on the surface of the implant prior to implantation, in order to mimic contamination during surgery as the infection route (Figure 1B).

2. Results and Discussion

2.1. Characterization of UPy-Modified SAAP-148GG in Solution

To assess whether the antimicrobial activity is affected by modifications of the peptide, the antimicrobial activity of the UPy-modified SAAP-148GG was assessed in solution. First,

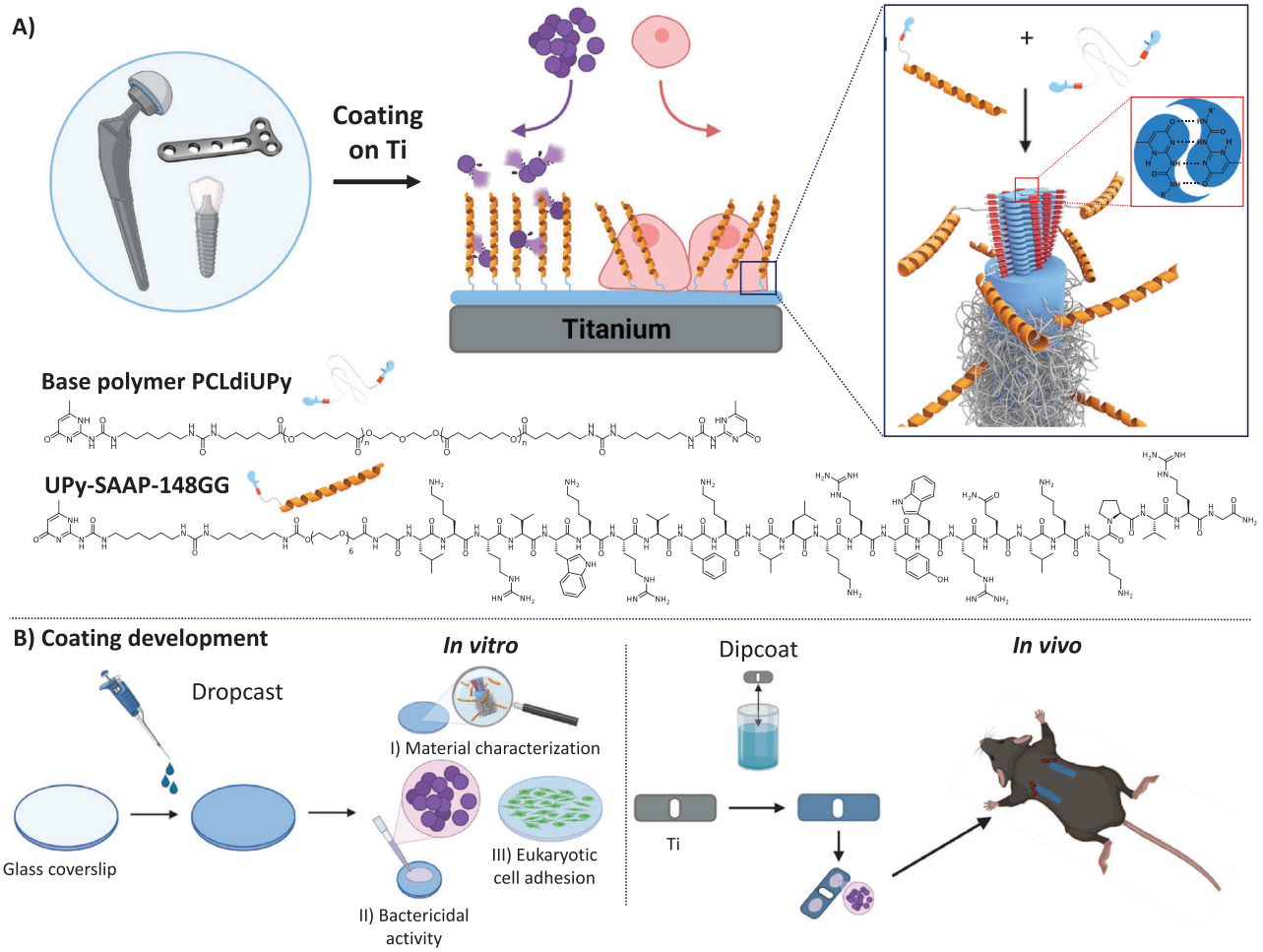

Figure 1. Development of an antimicrobial supramolecular coating on titanium based on the antimicrobial peptide SAAP-148GG. A) A coating for titanium implants is developed, which is antimicrobial but not toxic to eukaryotic cells. Schematic representation of the self-assembly of the base polymer PCLdiUPy and UPy-SAAP-148GG into nanofibers and the molecular structures of both molecules. B) Coating development via 1) a dropcast method on glass coverslips. Polymer films were used for material characterization and in vitro analyses, and 2) a dipcoat method on titanium implants. These coated implants were used to evaluate the coating performance in vivo.

SAAP-148GG was synthesized with solid phase peptide synthesis and coupled via the free N-terminal amine to a UPy-C_6-C_6-OEG_6-COOH linker (i.e., UPy-SAAP-148GG). The amphipathic nature of the cationic SAAP-148 complicated the UPy-coupling, which has been experienced before in the synthesis of other UPy-AMPs.[33] Therefore, an extra glycine was introduced at both the C- and N-terminus of SAAP-148 to enhance the yield of the synthesis (i.e., SAAP-148GG; Figure S1A, Supporting Information). Circular dichroism (CD) spectroscopy measurements showed that neither the addition of the extra glycines nor of the UPy-linker influenced the secondary structure of SAAP-148 (Figure S1B, Supporting Information). Even with both modifications, the molecule retained its α-helical structure which for α-helical AMPs is considered to be of crucial importance for their amphiphilicity and associated bactericidal activity.[38,39]

To assess whether the UPy-functionalization has an influence on the antimicrobial activity of the peptide, both the unmodified SAAP-148GG and UPy-SAAP-148GG were studied in vitro in Roswell Park Memorial Institute (RPMI) with and without 50% plasma against four (antimicrobial-resistant) bacterial patient strains of three species, namely, *S. aureus* JAR060131, the MDR strains *S. aureus* LUH14616[40] and *Acinetobacter baumannii* RUH875,[37] and an extended spectrum beta-lactamase (ESBL)-producing *Escherichia coli* strain.[41] The activity of the peptides against *E. coli* ESBL was not assessed in 50% plasma, because *E. coli* is killed in plasma by complement activation. Interestingly, no difference in activity between unmodified SAAP-148GG and UPy-SAAP-148GG was observed (**Table 1**). Both compounds were equally active at low micromolar concentrations against all four bacterial strains in RPMI (MIC_{RPMI} of 0.46×10^{-6} to 1.88×10^{-6} M and LC99.9 of 0.46×10^{-6} to 3.75×10^{-6} M after 2 h). However, upon addition of 50% plasma, both compounds had a reduced activity after 2 h (7.5×10^{-6} to 60×10^{-6} M) but were still able to kill the bacteria in 24 h at lower concentrations (MIC_{RPMI} and LC99.9 of 3.75×10^{-6} to 15×10^{-6} M). This shows that the bactericidal activity of SAAP-148GG is retained upon UPy-functionalization which is in line with results of previously synthesized UPy-AMPs in our group.[33] Next to the UPy-modification, the two extra glycines of SAAP-148GG did not influence its antimicrobial activity either, when compared to the

Table 1. Antimicrobial activity of SAAP-148GG and the modified UPy-SAAP-148GG in RPMI without and with 50% human plasma against the bacterial patient strains *S. aureus* JAR060131, MDR *S. aureus* LUH14616, MDR *A. baumannii* RUH875, and *E. coli* ESBL. Results are expressed as the lethal concentration (LC) 99.9%, which was the lowest concentration in μM at which ≥99.9% of the bacteria was killed at 2 and 24 h, and the minimal inhibitory concentration (MIC_{RPMI}), which represents the lowest concentration in μM at which no visible growth was observed after 24 h. All results are medians (and ranges) of two independent experiments with $n = 3$. If no range is indicated, all values were identical.

		S. aureus JAR060131		*S. aureus* LUH14616		*A. baumannii* RUH875		*E. coli* ESBL
		RPMI	50% plasma	RPMI	50% plasma	RPMI	50% plasma	RPMI
LC99.9 ($\times 10^{-6}$ M)		Defined as the lowest concentration of peptide ($\times 10^{-6}$ M) that killed 99.9% of an inoculum of 5.5×10^5 in 24 h.						
2 h	SAAP-148GG	1.4 (0.93–1.88)	60 (60–>60)	0.46	22.5 (15–30)	0.93 (0.46–0.93)	15 (15–30)	3.75 (1.88–7.5)
	UPy-SAAP-148GG	0.93	60 (30–60)	0.93 (0.46–0.93)	30	0.93 (0.93–1.88)	7.5 (7.5–15)	0.93
24 h	SAAP-148GG	0.93 (0.93–1.88)	11.3 (7.5–15)	0.46 (0.46–0.93)	3.75 (3.75–7.5)	0.93	7.5 (3.75–7.5)	1.88 (1.88–3.75)
	UPy-SAAP-148GG	0.93	15 (15–30)	0.93	15	1.88	3.75 (3.75–7.5)	1.88 (0.93–1.88)
MIC ($\times 10^{-6}$ M)		Defined as the lowest concentration of peptide ($\times 10^{-6}$ M) at which there is no visible bacterial growth after 24 h.						
24 h	SAAP-148GG	0.93	11.3 (7.5–15)	0.46	3.75 (3.75–7.5)	0.93	3.75	1.88 (1.88–3.75)
	UPy-SAAP-148GG	0.93	15 (15–30)	0.93	15	1.88	3.75	1.88 (0.93–1.88)

original SAAP-148 peptide, as no notable difference in MIC_{RPMI} or LC99.9 were observed (Table S1, Supporting Information).

2.2. Coating Development for Surface Characterization and In Vitro Antimicrobial Analysis

Next, the UPy-SAAP-148GG was formulated in the previously described supramolecular coating, by dropcasting either a solution of PCLdiUPy (control without peptide) or a solution of PCLdiUPy with 1 or 5 mol% UPy-SAAP-148GG on glass coverslips yielding dropcast polymer films (**Figure 2**E). The resulting polymer films all had the same thickness irrespective of the material composition (Figure 2D). The morphology of the dropcast films was probed with atomic force microscopy (AFM), in which the lighter domains in the phase images represent a harder phase in the film. In the zoomed phase images of 1 μm × 1 μm, the typical fiber structure of the self-assembly of the UPy moieties[28,42] was observed (Figure 2A). Upon addition of UPy-SAAP-148GG more hard, phase-separated domains (yellow regions) were observed at the surface, while the fiber morphology was still visible in the background. A higher peptide concentration led to more phase separation. Phase images for 5 mol% UPy-SAAP-148GG showed that the phase separation on the surface was not homogenous (Figure 2A).

The presence of the UPy-SAAP-148GG additive at the surface was also confirmed with X-ray photoelectron spectroscopy (XPS) measurements. Upon increase of the mol% of UPy-SAAP-148GG, an increase in nitrogen content was observed from 5.6 ± 0.6 for PCLdiUPy toward 8.2 ± 1.5 and 10.3 ± 0.5 atom percentage for 1 and 5 mol% UPy-SAAP-148GG, respectively (Figure 2B). This increase in nitrogen content can be explained by the introduction of peptide bonds and amino acids with UPy-SAAP-148GG. Besides this, the material surfaces became much more hydrophilic as indicated by the water contact angle (WCA). Upon addition of 1 mol% UPy-SAAP-148GG, the WCA dropped slightly from 69.8° ± 0.5° to 64.2° ± 0.6°. However, upon addition of 5 mol% UPy-SAAP-148GG, the WCA dropped much further to 39.3° ± 2.5° (Figure 2C). This increase in hydrophilicity was caused by the positively charged amino acids present in the UPy-SAAP-148GG. The standard deviation for the 5 mol% UPy-SAAP-148GG WCA measurements was higher compared to the other polymer films. This indicated again that the additive UPy-SAAP-148GG was not homogenously spread over the surface. In summary, all techniques used, confirmed the presence of the UPy-SAAP-148GG at the surface.

To assess the bactericidal activity of UPy-SAAP-148GG when immobilized in the dropcast polymer films, the JIS Z 2801:2000 surface microbicidal assay[43] was performed (Figure S2A, Supporting Information). In this assay, the same panel of bacterial patient strains was tested as previously used for the LC99.9 and MIC_{RPMI} studies. Glass coverslips and dropcast films of PCLdiUPy (without the additive UPy-SAAP-148GG) served as control, and showed growth of all four bacterial strains compared to the number of bacteria applied at the start of the experiment, which was ≈4.3×10^4 colony forming units (CFU) per sample (**Figure 3**). However, when 5 mol% UPy-SAAP-148GG was incorporated in the PCLdiUPy polymer films, nearly all bacteria were killed overnight. For the addition of 1 mol% UPy-SAAP-148GG, bacterial growth equal to the control samples was observed for *S. aureus* JAR060131, *A. baumannii* RUH875, and *E. coli* ESBL, while *S. aureus* LUH14616 did show reduced numbers of CFU on several of the polymer films. The variability that was observed between the different samples of this material could be explained by the inhomogenous surface coverage of UPy-SAAP-148GG on these polymer films as shown with AFM measurements. Apparently, 1 mol% was the limit value where, depending on the bacterial strain, either all bacteria were killed or a few survived, multiplied, and colonized the surface. Overall, incorporation of 1 mol% UPy-SAAP-148GG was not sufficient to create a generally bactericidal surface, while the higher concentration of 5 mol% UPy-SAAP-148GG was successful in killing all four (antimicrobial-resistant) bacterial patient strains.

Leakage studies of three individual samples per polymer film coating (0, 1, and 5 mol%) incubated in phosphate-buffered saline (PBS, 1 mL) for 24 h, revealed that not all of the UPy-SAAP-148GG was stably incorporated in the polymer films. For one of the 5 mol% polymer films tested, a maximum release of 17.5% (12.7 μg, 3.1 nmol, 3.1×10^{-6} M) was measured, while the other two polymer films showed a lower release which for one film was

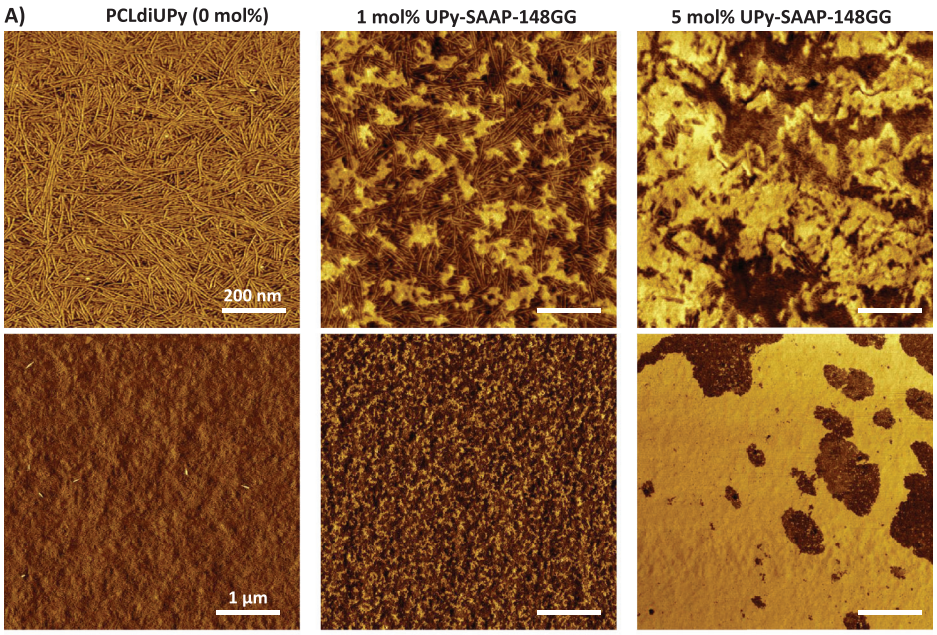

B)

Coating	C [%]	N [%]	O [%]
PCLdiUPy (0 mol%)	68.1 ± 1.7	5.6 ± 0.6	26.4 ± 1.0
1 mol% UPy-SAAP-148GG	65.8 ± 1.5	8.2 ± 1.5	26.0 ± 0.9
5 mol% UPy-SAAP-148GG	67.0 ± 0.8	10.3 ± 0.5	22.6 ± 1.2

C)

Coating	WCA (°)
PCLdiUPy (0 mol%)	69.8 ± 0.5
1 mol% UPy-SAAP-148GG	64.2 ± 0.6
5 mol% UPy-SAAP-148GG	39.3 ± 2.5

D)

Coating	Thickness (µm)
PCLdiUPy (0 mol%)	3.31 ± 0.25
1 mol% UPy-SAAP-148GG	3.43 ± 0.04
5 mol% UPy-SAAP-148GG	3.24 ± 0.09

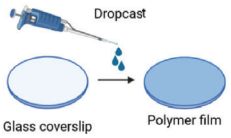

Figure 2. Surface characterization of the dropcast polymer films on glass coverslips with AFM, XPS, WCA, and profilometry. A) AFM phase images of the base polymer PCLdiUPy without (0 mol%) and with 1 or 5 mol% UPy-SAAP-148GG. The fibers represent the hard phase UPy-dimers in a soft phase polymer matrix. Top row scale bars represent 200 nm and bottom row 1 µm. B) XPS elemental composition of the different coatings, C) WCA of the different coatings, D) thickness of the different coatings measured with physical profilometry. Data are represented as mean of three measurements ± SD. E) Schematic representation of material preparation. Polymer films were created via dropcasting on glass coverslips.

equal to, and for the other was lower than the detection limit of 10 µg mL^{-1} (13%, 2.4 nmol, 2.4 × 10^{-6} M). This means that for two out of three samples release was measured, which in this volume would be enough to reach the bactericidal concentrations based on the LC99.9 and MIC data. No leakage was detected for the 1 mol% polymer films, indicating that the release was lower than the detection limit of 10 µg mL^{-1}. Due to this leakage from the polymer films, it remains unknown if the bacteria on these surfaces were killed by released peptide in solution, by direct contact killing at the surface, or via a combination of both. Release of UPy-SAAP-148GG will contribute to the coatings antimicrobial activity and may be beneficial in protecting the soft tissue surrounding an implant.

2.3. Dropcast Films for In Vitro Eukaryotic Biocompatibility Assays

It is known that AMPs at higher concentrations may lead to toxic side effects for eukaryotic cells.[33] The metabolic activity of normal human dermal fibroblasts (NHDFs) exposed to dropcast films of PCLdiUPy without the additive UPy-SAAP-148GG and PCLdiUPy with either 1 or 5 mol% UPy-SAAP-148GG was measured by performing a resazurin test, in which resazurin is converted to fluorescent resorufin by metabolically active cells. The morphology of the cells was similar in all groups and no distinct differences were observed in cell spreading (**Figure 4**A), although clearly lower numbers of cells were observed on the films with 5 mol% UPy-SAAP-148GG (Figure 4B). The lower number of cells also explains the lower metabolic activity per well which was observed on the 5 mol% UPy-SAAP-148GG films compared to activity of the cells on the PCLdiUPy films, suggesting that the remaining cells on the 5 mol% polymer films may have been similarly active as the cells on the control and 1 mol% UPy-SAAP-148GG polymer films (Figure 4C). The reduced cell numbers and therefore overall reduced metabolic activity per well with the 5 mol% polymer films, might be explained by a slightly toxic effect caused by UPy-SAAP-148GG released into the medium or by the presence of UPy-SAAP-148GG on the surface of the polymer film itself. Since the material properties such as the WCA of PCLdiUPy and 5 mol% UPy-SAAP-148GG polymer films differed considerably, this might have negatively influenced NHDFs adhesion as well.

The metabolic activity of the NHDFs cultured in the absence of fetal bovine serum (FBS) on the same dropcast films (Figure S3B, Supporting Information), and exposed to a concentration

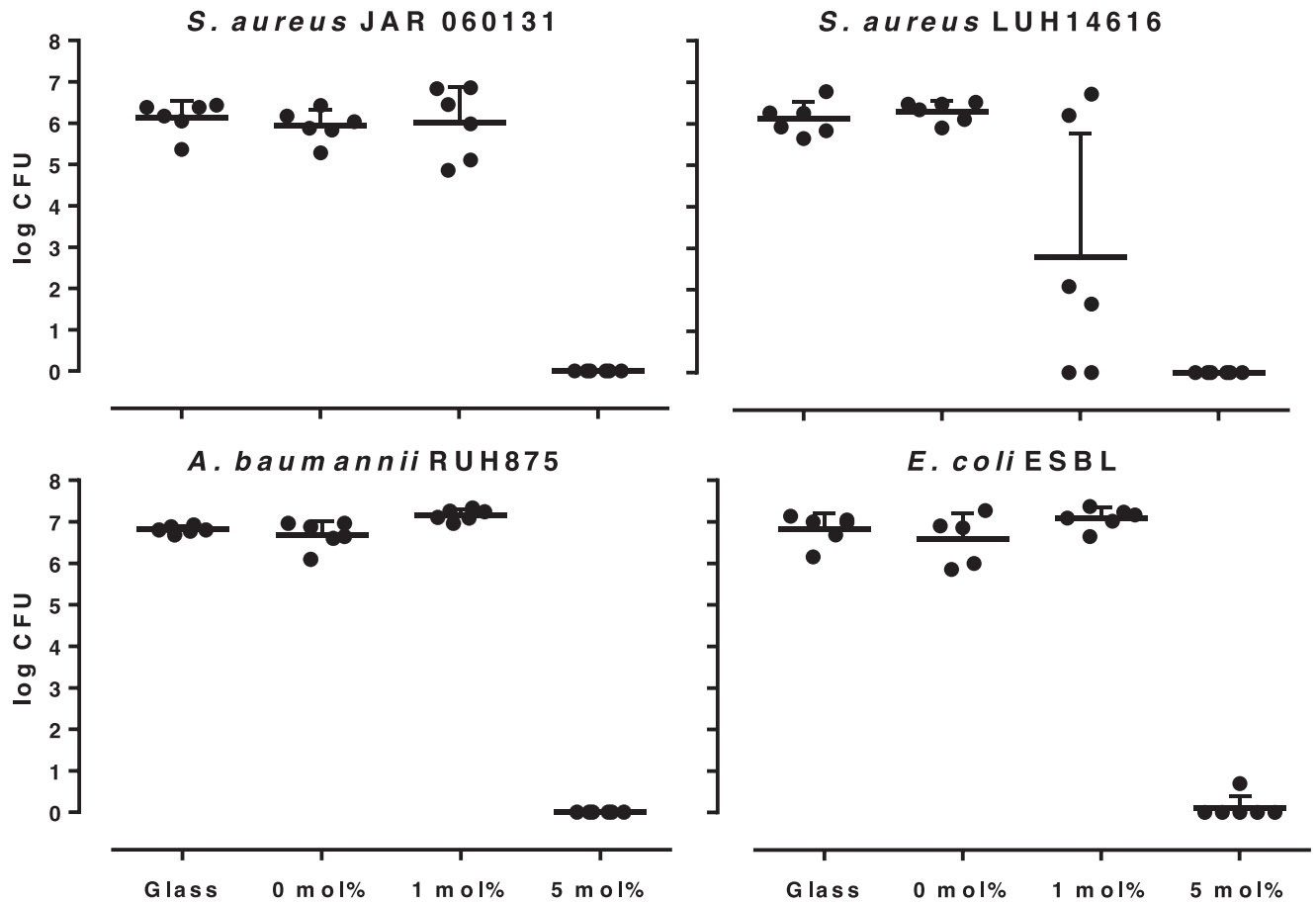

Figure 3. Surface bactericidal activity of glass, PCLdiUPy without (0 mol%) and with 1 or 5 mol% UPy-SAAP-148GG films determined via the JIS Z 2801:2000 assay. The materials were inoculated with ≈4.3 × 10^4 CFU per material. Data represent mean ± SD of two independent experiments with both $n = 3$.

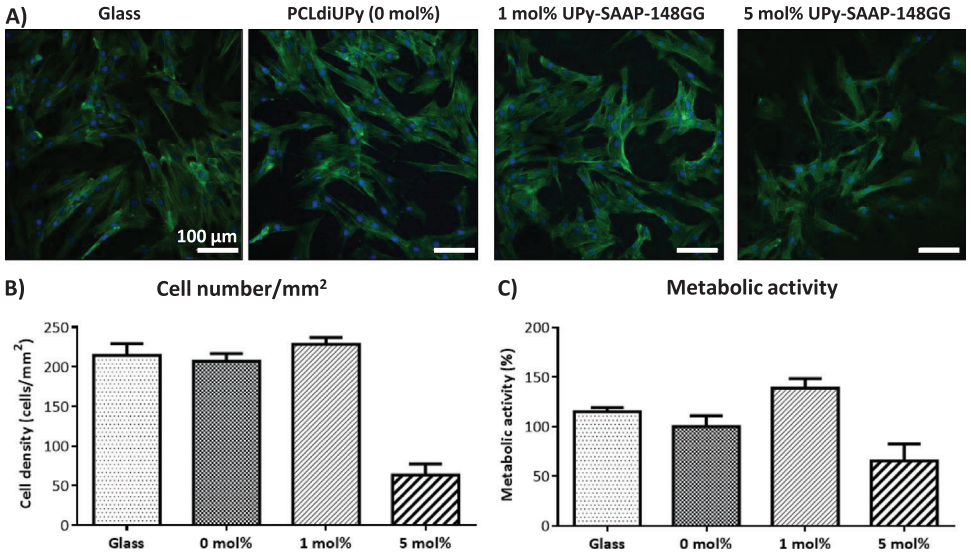

Figure 4. Cell morphology, numbers, and metabolic activity for normal human dermal fibroblasts cultured in the presence of FBS on glass coverslips, PCLdiUPy without (0 mol%) and with 1 or 5 mol% UPy-SAAP-148GG. A) NHDF cells cultured on the different materials for 24 h. Cells were stained for nuclei (blue) and actin cytoskeleton (green), and scale bars represent 100 µm. B) The number of adhered cells per mm^2 was determined at three locations per substrate through nuclei counting. $n = 3$ per condition, data are depicted as mean ± SEM. C) Metabolic activity was determined through resazurin conversion. Results were normalized to PCLdiUPy without peptide (0%). $n = 6$ per condition, data are depicted as mean ± SEM.

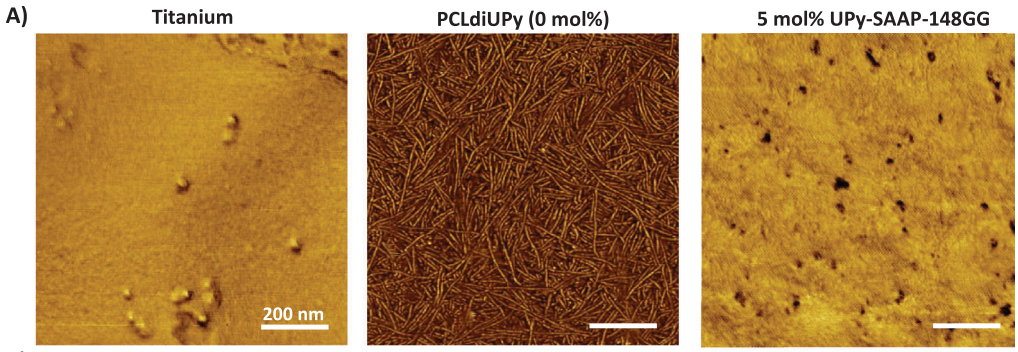

B)

Surface	C [%]	N [%]	O [%]	Ti [%]
Titanium	57.9 ± 4.0	1.8 ± 0.3	34.3 ± 3.5	6.0 ± 0.9
PCLdiUPy	70.4 ± 2.9	4.5 ± 0.6	25.2 ± 2.3	0.0 ± 0.0
5 mol% UPy-SAAP-148GG	67.1 ± 1.3	8.6 ± 1.1	24.3 ± 0.3	0.0 ± 0.0

C)

Surface	WCA (°)
Titanium	75.0 ± 1.3
PCLdiUPy (0 mol%)	76.6 ± 1.9
5 mol% UPy-SAAP-148GG	23.9 ± 3.7

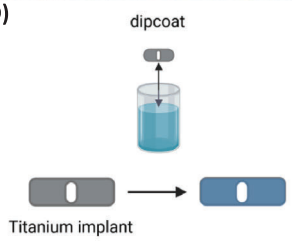

Figure 5. Surface characterization of the polymer films on titanium implants. A) AFM phase images of the uncoated titanium implant, the PCLdiUPy-coated implant (0 mol%), and the PCLdiUPy with 5 mol% UPy-SAAP-148GG-coated implant, respectively. Scale bars are 200 nm. B) XPS elemental composition of the different coatings, C) WCA of the (coated) titanium implants. Data are represented as mean of three measurements ± SD. D) Schematic representation of material preparation; polymer films were prepared via dipcoating of the titanium implants.

series of SAAP-148GG and UPy-SAAP-148GG in solution (Figure S3A, Supporting Information), showed that there is no difference in cytotoxicity between SAAP-148GG and UPy-SAAP-148GG. Moreover, in the absence of FBS, the 1 and 5 mol% UPy-SAAP-148GG films induced cell adhesion (Figure S3C, Supporting Information), however, with reduced metabolic activity at the 5 mol% UPy-SAAP-148GG films (Figure S3D, Supporting Information).

Overall, the NHDFs do show a spread cell morphology on all polymer films and the cells remain metabolically active. The slight reduction in metabolic activity at the 5 mol% UPy-SAAP-148GG films can be explained by the reduction in number of cells per mm^2 (i.e., cell density). Thus, the cells are not affected in their metabolic activity, but seem to attach less. In the future, initial cell adhesion on these polymer films could be improved by incorporation of biological adhesion cues such as cRGD.[44,45] Moreover, earlier toxicity studies with SAAP-148 demonstrated a lack of cytotoxicity for cells in a human skin model but only for human skin cells in 2D culture, as mentioned before. Therefore, despite the reduced cell adhesion observed in vitro, applications for use in vivo still have potential.[46] In conclusion, because of the high antimicrobial activity, the normal morphology of the NHDFs attached on the surface and their normal metabolic activity per cell, the 5 mol% UPy-SAAP-148GG was selected for further characterization in a murine implant infection model.

2.4. Material Characterization of Dipcoat Titanium Implants

Due to the more challenging and complex 3D shapes of implants and medical devices, dropcasting is not suitable to coat such devices. Therefore, a dipcoating technique was used for titanium implants to be used in a subcutaneous mouse implant infection model, which allowed full coating coverage of complex-shaped implants. During the dipcoating procedure, the solid titanium implants were dipped in an automated fashion into a polymer solution of either only PCLdiUPy (i.e., 0 mol%) or PCLdiUPy with 5 mol% UPy-SAAP-148GG and left to dry which resulted in implants coated with a polymer film (**Figure 5**D). The thickness of the polymer film was estimated to be around ≈3 µm but could not exactly be determined due to the surface roughness of the titanium implants.

The material properties of the coating were again evaluated with surface characterization techniques. AFM results showed that the titanium implants were fully covered by the PCLdiUPy polymer films and upon addition of 5 mol% UPy-SAAP-148GG, harder domains were observed in line with the observations for the dropcast coatings (Figure 5A). The chemical composition of the (coated) implants determined with XPS showed a titanium signal of 6.0 ± 0.9 atom% for the uncoated titanium implants, which completely disappeared once the implants were coated indicating again a full surface coverage of the implant surface (Figure 5B). Besides this, the addition of UPy-SAAP-148GG resulted in a higher percentage of nitrogen atom% due to the extra peptide bonds and amino acids. Finally, the WCA dropped dramatically from 76.6° ± 1.9° for PCLdiUPy-coated surfaces to 23.9° ± 3.7° for the surfaces coated with polymer films containing 5 mol% UPy-SAAP-148GG (Figure 5C). Overall, no striking differences between the dropcast polymer films on glass coverslip and dipcoat polymer films on titanium were observed. Further research should involve assessment of resistance to degradation of the coatings by physical, mechanical, (bio)chemical, and biological agents, an important aspect for clinical application of these coating, for instance at the surface of orthopedic devices.

2.5. Antimicrobial Activity of Dipcoated Polymer Films—Optimization for In Vivo Study

The bactericidal activity of the dipcoated polymer films was assessed with a pre-seeding method that corresponds with the procedure for administering the bacteria in the in vivo experiment (Figure S2B, Supporting Information). The biggest difference compared to the JIS assay was the higher inocula used here and drying of the inoculum in air after application on the polymer films. Here, *S. aureus* JAR 060131 was selected, as it was originally isolated from a patient with an orthopedic device-related infection.[47,48]

First, the influence of the coating fabrication method was investigated by comparison of dropcast and dipcoated polymer films on glass coverslips. No differences between dropcast and dipcoated polymer films were observed (Figure S4A, Supporting Information). However, drying of the inoculum which was part of the test procedure did affect bacterial viability. The 5 mol% UPy-SAAP-148GG-coated samples showed reduced numbers of CFU already directly after drying, i.e.. after ≈10 min, and complete killing overnight (Figure S4A, Supporting Information). This indicates that with this method 10–100-fold reduction in numbers of bacteria was already observed, but no full killing was reached yet at the time of implantation. For the in vivo experiments, an inoculum of 2×10^5 (per side) was chosen since it is within the range of the capacity of the coating and similar to other studies.[49]

Two different sterilization methods for the coated implants were compared, ultraviolet C (UV-C) light irradiation versus ethylene oxide (EtO) sterilization. UPy-SAAP-148GG became (partly) antimicrobially inactive after sterilization with EtO (Figure S4B, Supporting Information). The inactivation was caused by chemical modification of UPy-SAAP-148GG after EtO sterilization as revealed by liquid chromatography-mass spectrometry (LC-MS) analysis (Figure S5E, Supporting Information). This has been reported for other peptides in literature before.[50,51] Furthermore, an increase in WCA for the EtO sterilized surfaces was observed, when compared to the UV-C sterilized surfaces (Figure S5D, Supporting Information), which also was indicated by changes in the phase image (Figure S5B, Supporting Information) and chemical composition (Figure S5C, Supporting Information). Therefore, in the in vivo study, the 5 mol% UPy-SAAP-148GG implants were sterilized by UV-C, and showed complete killing of *S. aureus* JAR 060131 (Figure S4B, Supporting Information), while the uncoated titanium and PCLdiUPy-coated implants were sterilized with EtO which has been used for the sterilization of supramolecular materials before.[52]

2.6. Antibacterial Activity of PCLdiUPy Polymer Films with 5 mol% UPy-SAAP-148GG on Titanium Implants in a Mouse Experimental BAI Model

The in vivo efficacy of the PCLdiUPy with 5 mol% UPy-SAAP-148GG coating on titanium implants was assessed in the murine subcutaneous implant infection model. First, colonization of the implants as well as of the peri-implant tissue by *S. aureus* JAR060131 at 1 day after inoculation and implantation was determined. Mice either received noncoated, PCLdiUPy (i.e., 0 mol% UPy-SAAP-148GG) or PCLdiUPy with 5 mol% UPy-SAAP-148GG-coated titanium implants subcutaneously. An *S. aureus* JAR060131 inoculum of 4×10^5 CFU (two droplets of each 2×10^5, Figure S2B, Supporting Information) was pre-seeded on the (coated) implants and air-dried for ≈10 min prior to implantation. At 1 day after challenge, both the implants and tissues from the control mice (having received either noncoated or PCLdiUPy-coated titanium implants) did not differ in frequency of culture positive samples nor in the number of CFU cultured from these implants and surrounding tissues (**Figure 6**A). This proved that the PCLdiUPy polymer film itself had no antimicrobial activity. Implantation of implants coated with the PCLdiUPy containing 5 mol% UPy-SAAP-148GG resulted in a significantly lower percentage of culture-positive implants (13%) than for the noncoated (100%; $p < 0.001$) and PCLdiUPy-coated implants (94%; $p < 0.001$). Moreover, mice receiving the implants coated with the PCLdiUPy polymer films with 5 mol% UPy-SAAP-148GG had a significant 4.5-log ($p < 0.001$) and 4.3-log ($p < 0.001$) reduction in numbers of CFU on the implant surface when compared to the noncoated and PCLdiUPy-coated implants, respectively. Similarly, a more than 3-log reduction in numbers of CFU was observed in the sample of the tissues surrounding the UPy-SAAP-148GG implants when compared to the control groups ($p < 0.001$ for both). Both in the tissue and on the implants of the control groups, an increase in CFU numbers relative to the inoculum was observed, while reduced numbers of CFU were retrieved from the UPy-SAAP-148GG implants. Neither apparent macroscopic signs of toxicity or inflammation were observed in any of the mice after explantation of the coated implants, nor did the animals show behavior suggestive of discomfort of any kind. Thus, the SAAP-148GG-functionalized polymer film protected titanium implants from surface colonization by *S. aureus*, and also reduced the tissue colonization around the implants at 1 day after challenge, without signs of toxicity.

During surgery, bacteria may adhere to the implant and initiate biofilm formation. Bacteria adherent to or in a biofilm on the implant are a potential source of infection, acting as a reservoir for infection of the surrounding tissue where bacteria can even reside intracellularly.[9] In this study, the bacteria were pre-seeded on the implant surface to mimic the assumed major contamination route during surgery. To examine whether bacteria which "escaped" into the peri-implant tissue would decrease in numbers or multiply, the colonization of both implant and tissue at 4 days after challenge was assessed in a follow-up experiment. As the PCLdiUPy coating itself in the previous experiment had not shown any antimicrobial activity nor toxic effects, we did not test this "empty" coating for this 4 days time point, in order to minimize the numbers of mice.

At 4 days after challenge, the PCLdiUPy polymer film containing 5 mol% UPy-SAAP-148GG again caused a significantly lower percentage of culture-positive implants (28%) than the noncoated implants (89%; $p < 0.001$), and in a significant 3.7-log ($p < 0.001$) and 6-log ($p < 0.01$) reduction in median numbers of CFU on the implant surface and in the surrounding tissue, respectively, when compared to the noncoated implants (Figure 6B). These results showed that the UPy-SAAP-148GG-based coating was also able to further reduce tissue colonization over time and underline the importance of novel antimicrobial strategies to prevent both biofilm formation and tissue colonization. Pre-operative

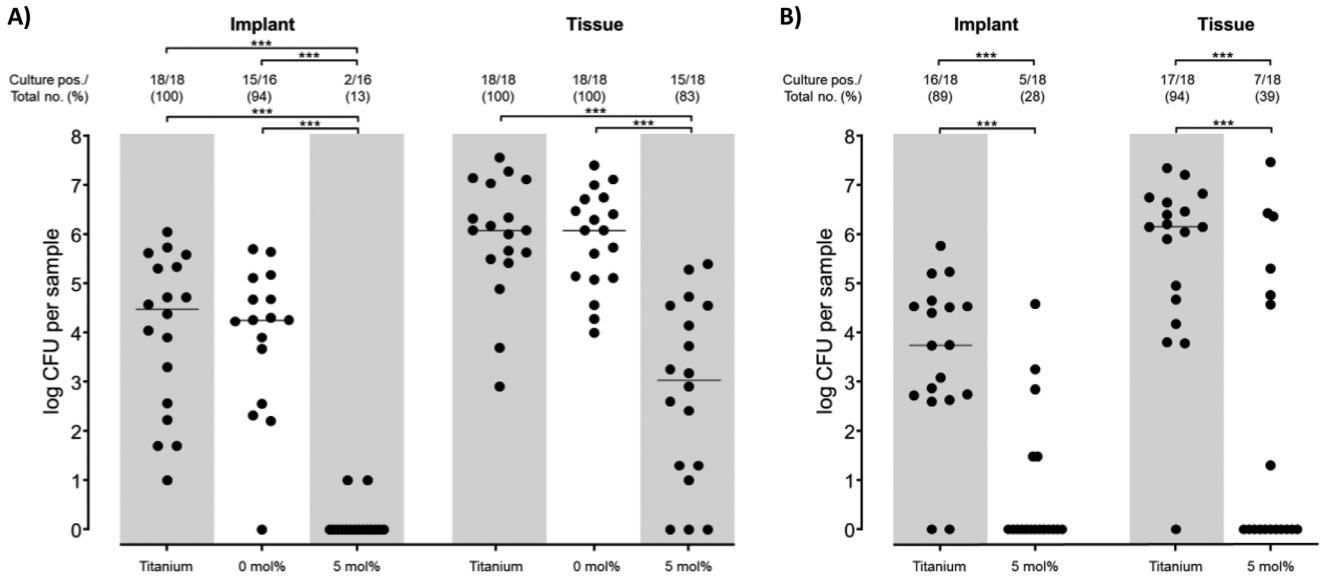

Figure 6. Bacterial colonization of (coated) implants and peri-implant tissue in mice expressed as the fraction (and percentage) of culture-positive samples, and as the actual numbers of CFUs retrieved. Inocula of 4×10^5 CFU of *S. aureus* JAR060131 were pre-seeded onto the implant prior to implantation. The survival of bacteria on the implant and in the tissue surrounding the implant is shown as log CFU at A) 1 day and B) 4 days after implantation. The horizontal line represents the median value per group. Statistical analyses showed a significant difference between the indicated conditions with $p < 0.001$.

antibiotic prophylaxis is known to reduce the risk of BAI, but in some cases antibiotics fail to eradicate all infecting bacteria. Local protection, by coating the implant directly, in combination with prophylaxis might further reduce the infection rates after implantation of biomaterials such as orthopedic prostheses.

Our results showed that *S. aureus* bacteria on the (noncoated) surface of titanium implants are a source of infection of the surrounding tissue, even when the bacteria were inoculated exclusively on the implant surface at the start of the mouse study. It should be noted though, that culture positivity of tissue samples may partially be due to bacteria from a biofilm formed at the interface of implant and tissue, which partially may be attached to the tissue when implant and surrounding tissue are separated during sample preparation for culture. We have however in many previous studies observed *S. epidermidis* and *S. aureus* abundantly within the peri-implant tissue and within host (immune) cells.[6,9,13,53] In a murine experimental BAI model, *S. epidermidis* persists in peri-implant tissue rather than on the implanted biomaterial itself,[54,55] despite rifampicin/vancomycin treatment.[56] Moreover, viable *S. epidermidis* bacteria could be visualized in the tissue surrounding intravascular devices of deceased patients.[57] The presence of bacteria in peri-implant tissue is an important factor in the pathogenesis of BAI, and should therefore be taken into account when designing preventive strategies. Although a contact-killing coating only eradicates bacteria that are in direct contact with the implant surface, this strategy might still be sufficient to prevent peri-implant tissue colonization owing to the effective killing early upon implantation. To ensure sufficient killing of all bacteria not directly associated with the surface of the material, but in the surrounding tissue as well, a coating with combined surface and released microbicidal activity might be preferred. The potency of such a strategy was shown by a dual-functional coating with initial bacteria-killing efficiency due to the release of Ag^+ ions and retained antibacterial activity after the depletion of embedded Ag^+ because of the immobilized quaternary ammonium salts.[58] Similar results were obtained using AMPs: modifying polydimethylsiloxane with both covalently bound AMPs and drug-eluting capabilities resulted in both contact-killing and released activity, respectively.[59] Moreover, the AMP GL13K immobilized onto titanium exhibited strong contact- and release-killing abilities.[60] Since the developed PCLdiUPy coating with 5 mol% UPy-SAAP-148 also showed some release of the UPy-SAAP-148GG, this antimicrobial coating may provide this desired combined strategy in the fight against BAI. This supramolecular approach makes it possible to coat complex-shaped implants and using the UPy moiety allows incorporation of a selection of antimicrobial agents and cell instructive molecules, thereby making it a very versatile technique that can be personalized to the patient's needs.

3. Conclusion

With the use of supramolecular interactions, an antimicrobial coating on titanium was developed which allowed for the presentation of SAAP-148GG. In vitro studies on the antimicrobial activity showed that 5 mol% UPy-SAAP-148GG containing polymer films were able to kill (multidrug-resistant) bacteria. Moreover, in vivo peri-implant tissue colonization in mice was significantly reduced. We have demonstrated that using supramolecular chemistry a promising alternative peptide-based contact-killing and release coating on titanium has been developed which can be used to prevent BAI. The development of these AMP-functionalized supramolecular antimicrobial coatings has great significance in guiding the design of novel antimicrobial coating in the post-antibiotic era.

4. Experimental Section

Materials: PCLdiUPy,[45] UPy-C_6-C_6-OEG_6-COOH,[61] and UPy-C_6-C_{12}-OEG_{12}-COOH were synthesized by SyMO-Chem BV (Eindhoven, The Netherlands). SAAP-148 was synthesized by the department of Immunohematology and Blood Transfusion, Leiden University Medical Center (Leiden, The Netherlands). Solid medical grade (ISO 5832/11) titanium implants (10 × 4 × 1 mm, with a slit to allow cutting the implants after explantation) were machined at AO Research Institute (Davos, Switzerland) and anodized in the final processing step at KKS Ultraschall AG (Steinen, Switzerland). Unless stated differently, chemicals were purchased from Sigma-Aldrich.

Synthesis of SAAP-148GG: SAAP-148[37] was synthesized by automated Fmoc-based solid phase peptide synthesis (SPPS). An extra glycine was introduced on both the C- and N-terminus, resulting in the amino acid sequence: GLKRVWKRVFKLLKRYWRQLKKPVRG and is referred to as SAAP-148GG. The peptide was synthesized on an Fmoc-Sieber-TentaGel resin (Iris Biotech), 0.19 mmol g^{-1} in batches of 10 µmol scale with dimethylformamide (DMF) as solvent. As coupling system 2-(1*H*-benzotriazol-1-yl)-1,1,3,3-tetramethyluronium hexafluorophosphate (HBTU) in combination with *N*,*N*-diisopropylethylamine (DIPEA) was used in 1:1:4 molar equivalents of amino acid:HBTU:DIPEA. The amino acids (Novabiochem) were added in four times excess compared to the resin. A drop of Triton-X100 was added to each amino acid solution to prevent peptide aggregation. All couplings were performed in duplicate for 30 min. Fmoc deprotection was achieved with a 20% v/v solution of piperidine in DMF, two times for 10 min. After each coupling, a capping step with pyridine:acetic anhydride:DMF (1:1:3 v/v/v) solution was performed for 8 min. The resin was washed with DMF in between all steps. After coupling of the last amino acid, the Fmoc was deprotected yielding a peptide with a free amine N-terminus.

Subsequently, the SAAP-148GG peptide was checked for successful synthesis with reversed phase high pressure liquid chromatography mass spectrometry (RP-HPLC-MS) with a reverse phase C18 column and a linear gradient of 5–95% acetonitrile (ACN)/H_2O with 0.1% trifluoroacetic acid (TFA).

After successful synthesis, 40 µmol of the batch was cleaved from the resin with 92.5% TFA, 2.5% triisopropylsilane (TIS), 2.5% dH_2O, and 2.5% 1,2-ethaneditihol (EDT) (v/v) for 3 h at room temperature. The rest of the synthesis batch was used for coupling with the UPy-COOH synthon. After cleavage, the TFA was evaporated using a nitrogen-flow after which the cleaved peptide was precipitated in ice-cold diethylether, centrifuged at 2600 rpm for 5 min, dissolved in ACN/H_2O (1:6, v/v) and lyophilized. After filtration, the SAAP-148GG peptide was purified with an RP-HPLC-MS system and reverse phase C18 column with a linear gradient of 34–39% ACN/H_2O with 0.1% TFA. All fractions were collected and lyophilized again. Subsequently, the lyophilized purified product was dissolved in 4 × 10^{-3} M HCl to reduce the TFA counter ion and lyophilized once more resulting in an overall yield of 11.4% (15.2 mg, 4.5 µmol) with 95% purity. With Fluorine-19 NMR spectroscopy (F-NMR) on a Bruker UltraShield 400 MHz spectrometer, the residual presence of TFA was checked. SAAP-148 was dissolved at 4 mg mL^{-1} in D_2O and potassium hexafluoro phosphate was added as reference compound (4 mg mL^{-1}). Comparison of the integrals demonstrated that there was 0.004 TFA ion present per SAAP-148GG molecule (Figure S6, Supporting Information). The purified SAAP-148GG was stored at −30 °C. ^{19}F NMR (376 MHz, D_2O, δ): 72.2 (d, KPF_6), 75.6 (CF_3COOH). RP-HPLC-MS: calc exact mass = 3337.1 g mol^{-1}, found *m*/*z*: 1669.5 $[M+2H]^{2+}$, 1113.9 $[M+3H]^{3+}$, 835.9 $[M+4H]^{4+}$.

Coupling of UPy-COOH to SAAP-148GG: After the peptide synthesis, the 10 µmol batches were collected together in one syringe to manually couple the UPy linker. To one-third of the SAAP-148GG batch, an UPy-C_6-C_6-OEG_6-COOH linker was coupled in 2 equivalents to the N-terminus of the peptide (1 eq.). The UPy-coupling was performed while the peptide was still protected and on the resin, using 1-[bis(dimethylamino)methylene]-1*H*-1,2,3-triazolo[4,5-*b*]pyridinium 3-oxide hexafluorophosphate (HATU; 2 eq.) and DIPEA (10 eq.) in DMF at room temperature, overnight. Next, the UPy-SAAP-148GG was deprotected and cleaved from the resin with the cleavage mixture of TFA/TIS/dH_2O/EDT (95/2.5/2.5/2.5% v/v) for 3 h at room temperature. The TFA was removed with a flow of nitrogen and the UPy-peptide was precipitated in ice-cold diethylether. Next, the solution was centrifuged at 2600 rpm for 5 min and the pellet was dissolved in dH_2O and lyophilized obtaining a white powder. After filtration, the UPy-SAAP-148GG was purified on an RP-HPLC-MS system with a reverse phase C18 column, using a linear gradient of 40–45% ACN/H_2O with 0.1% TFA. All fractions were collected and lyophilized. Subsequently, the same protocol as described before to remove the TFA counter ion was executed, and F NMR measurement revealed there were still 3.4 TFA ions present per UPy-SAAP-148GG molecule (Figure S7, Supporting Information). The final product had a purity of >99% and was obtained in a yield of 8.5% (104.4 mg, 25.5 µmol). The purified UPy-SAAP-148GG was stored at −30 °C. ^{19}F NMR (376 MHz, D_2O, δ): 72.2 (d, KPF_6), 75.6 (CF_3COOH). RP-HPLC-MS: calc exact mass = 4094.5 g mol^{-1}, found *m*/*z*: 1366.2 $[M+3H]^{3+}$, 1025.1 $[M+4H]^{4+}$, 820.3 $[M+5H]^{5+}$, 683.8 $[M+6H]^{6+}$.

Bacterial Cultures: The patient strains *S. aureus* JAR060131, obtained from a patient with an orthopedic device-related infection,[47,48] the multidrug-resistant (MDR) *S. aureus* LUH14616[40] and *A. baumannii* RUH875[37] and the extended-spectrum β-lactamase (ESBL)-producing *E. coli* strains[41] were used in the present study. Prior to each experiment, bacteria from frozen stocks were grown overnight at 37 °C on sheep blood agar plates (BioMerieux).

Antimicrobial Activity in Solution: The bacteria were cultured to mid-logarithmic growth phase in tryptic soy broth (TSB; Oxoid) at 37 °C and 130 rpm, pelleted, washed once with PBS (pH 7.4), resuspended and diluted in modified RPMI-1640 medium (with 20 × 10^{-3} M Hepes and L-glutamine, without sodium bicarbonate) to 1 × 10^7 CFU mL^{-1}, based on the optical density of the suspension at 620 nm (OD_{620}). 10 µL of this bacterial suspension (final concentration of 1 × 10^6 CFU mL^{-1}) was added to 90 µL peptide [final concentrations of 0.06 × 10^{-6} to 60 × 10^{-6} M] in RPMI without or with a final concentration of 50% v/v pooled human plasma (Sanquin, The Netherlands) in polypropylene flat bottom microtiter plates (Greiner). As nontreated control, bacteria were incubated without peptides in RPMI or RPMI with 50% plasma. All conditions were performed in triplicate. The plates were incubated for 2 h and overnight at 37 °C and 200 rpm.

After 2 h of incubation, a 20 µL sample was taken from the incubation and added to 20 µL of PBS containing 0.05% v/v sodium polyanethole sulfonate (SPS) to neutralize peptide activity.[62] Subsequently, 10 µL aliquots of the neutralized solution were plated on blood agar plates to determine the number of viable bacteria. After overnight incubation, the wells were visually inspected for growth and the minimal inhibitory concentration (MIC_{RPMI}), i.e., the lowest concentration without visible growth, was determined. Moreover, 10 µL aliquots were directly plated on blood agar plates to determine the number of viable bacteria. The blood agar plates were inspected for growth after overnight incubation at 37 °C. Antimicrobial activity is expressed as the 99.9% lethal concentration (LC99.9), i.e., the lowest peptide concentration that killed ≥99.9% of the inoculum after 2 h or overnight of incubation. All experiments were performed at least in duplicate with $n = 3$, with exception of the SAAP-148 and SAAP-148GG comparison study, which was performed once with $n = 2$. Of note, the activity against *E. coli* was not assessed in plasma, as this strain proved to be plasma sensitive.

CD Measurements: Samples for CD measurements were prepared at 50 × 10^{-6} M concentrations in either ultrapure water or 30 × 10^{-3} M sodium dodecyl sulfate.[63] The spectra were recorded from 190 to 250 nm, at 25 °C using a path length of 0.1 cm and a bandwidth of 2 nm. The spectra were obtained by averaging three scans. The molar residual ellipticity was determined using the following equation[64]: $[\theta] = \frac{\theta \times m}{C \times l \times n_2}$, where θ is the ellipticity in millidegrees, m is the molecular weight in g mol^{-1}, c is the concentration in mg mL^{-1}, l is the path length in cm, and n_2 is the number of amino acids in the peptide.

Preparation of Dropcast Films: Solutions of PCLdiUPy were prepared at 7.1 × 10^{-3} M (20 mg mL^{-1}) in hexafluoro-2-propanol (HFIP). The UPy-SAAP-148GG was dissolved at a concentration of 7.1 × 10^{-3} M in HFIP. These solutions were mixed in molar ratios of PCLdiUPy:UPy-SAAP-148GG of 99:1 or 95:5 obtaining either 1 or 5 mol% UPy-SAAP-148GG samples. Dropcast films were prepared by casting 50 µL of the polymer

solutions on glass coverslips (Ø 14 mm; Menzel-Gläser). The polymer films on the glass coverslips were air-dried for 1 h before drying in vacuum overnight. The casting was performed in a relative humidity of around 40%. This yielded in thin transparent films of around 3.3 µm thickness.

Preparation of Dipcoat Films: Solutions of PCLdiUPy were prepared at 35.6×10^{-3} M (100 mg mL^{-1}) in HFIP. The UPy-SAAP-148GG was dissolved at the same concentration of 35.6×10^{-3} M in HFIP. These solutions were mixed in molar ratios of PCLdiUPy:UPy-SAAP-148GG 95:5 obtaining a 5 mol% UPy-SAAP-148GG solution. The solid titanium implants were dipcoated using a Dip Coater (Ossila) with 9 mm s^{-1} dip speed, 5 s dwell time, 4 mm s^{-1} withdrawal time, and 1 dip cycle. Small 0.55 mm diameter needles (nr. 17; BD microlance) were bended into a hook-shape and served as dipping probe for the implants. With use of the hook-shape needle, the contact area between the dipping probe and the implant was minimized and located at the inside of the implant, resulting in a minimal noncoated surface area. The dipcoated implants were air-dried for 15 min, before drying in vacuum overnight. The dipcoating was performed in a relative humidity of around 40%. This yielded in a transparent coating of ≈3 µm thickness. One of the dipcoated titanium implants was submerged in water to assess its stability and the coating remained firmly attached to the titanium implant.

UPy-SAAP-148GG Extraction from Dipcoat Films after Sterilization: Dipcoated titanium implants were either sterilized with UV-C irradiation (15 min) or EtO (Synergy Health, The Netherlands). The sterilized dipcoated implants were submerged in 500 µL chloroform, and shaken at 1000 rpm for 30 min to dissolve the dipcoated polymer coating. After 30 min, 500 µL milliQ was added, and shaken at 1000 rpm for 5 min. Both solutions were left to phase separate and the water-phase was measured with LC-MS with a reverse phase C18 column and a linear gradient of 5–95% acetonitrile (ACN)/H_2O).

Atomic Force Microscopy (AFM): AFM was performed at room temperature using either a Digital Instrument Multimode Nanoscope IV or a Digital Instrument Dimension 3100 Nanoscope IIIa, operating in tapping regime mode using silicon cantilever tips (PPP-NCHR, NanoSensors, 204–497 kHz, 10–130 N m^{-1}). Height and phase images of the dropcast and dipcoated films were recorded in air. The images were processed with Gwyddion software (version 2.52).

XPS Measurements: XPS spectra of the samples were measured using a Thermo Scientific K-Alpha spectrometer equipped with a monochromatic, small-spot X-ray source and a 180° double-focusing hemispherical analyzer with a 128-channel detector using an aluminum anode (Al Kα, 1486.7 eV, 72 W). Region scans of the individual atoms (C, N, O, and Ti) were recorded using pass energies of 50 eV. In total three spots on the surface of a sample were measured and data were represented as mean ± standard deviation. The analysis and quantification of the spectra was performed using CasaXPS software (version 2.3.23).

WCA Measurements: WCA was determined at room temperature in air using an OCA 30 (DataPhysics). Ultrapure water droplets of 2 µL were dispensed with a speed of 2 µL s^{-1}. The angle of the droplet on the polymer–water–air interface was measured 5 and 30 s after deposition of the droplet on the surface using SCA20_U software. For the dropcast films, three droplets were dispensed over three replicates, for the dipcoated implants two droplets were dispensed over three replicates. No dynamic response or change of WCA was observed between the time points, and therefore only the results of the 5 s time point were reported.

Profilometer Measurements: The thickness of the polymer films was measured with a physical profilometer (DEKTAK; Veeco Instruments Inc.) and software DEKTAK version 9.0.76. A scratch was made manually in the polymer dropcast films and the height difference of the scratch compared to the polymer surface was measured with a 12.5 µm stylus, using a 3.00 mg force. Both hills and valleys were recorded with a meas range of 6.5 µm, scan length of 600 µm, and scan duration of 15 s. The meas range is the range of the instrument for which the error of the measurement is within the limits, indicating that the measurement has a well-defined accuracy.

It was not possible to scratch only the polymer surface at the dipcoated implants. Therefore, a corner of the sample was taped during dipcoating. Upon removal of the tape, the thickness of the coated layer was determined with a meas range of 65.5 µm, scan length of 1200 µm, and scan duration of 30 s. This yielded in a resolution of 0.067 µm per sample for both the dropcast and dipcoated samples. The height difference of the scratches was measured at room temperature for three replicates per condition. The final thickness of the polymer film was presented as the average step height (ASH) ± the standard deviation.

Leakage Experiments: Glass coverslips coated with polymer films were placed in wells of a 24 well-plate (Corning Costar) in triplicate and incubated with 1 mL PBS at 37 °C for 24 h. After incubation, the solution was removed from the surface and enriched with 0.1% v/v formic acid. The samples were analyzed on an LC-MS system with a reverse phase C18 column. The total ion count, which is represented by the surface area of the peak was calculated with the ICIS algorithm. The results were fitted to a calibration curve determined of samples with 0.1, 0.05, 0.01, 0.001, 0.0001 mg mL^{-1} concentration. Due to the sticky nature of the UPy-SAAP-148GG to the LC-MS column, the detection limit of the system was limited to 0.01 mg mL^{-1}. The lowest two concentrations of the calibration curve could not be detected anymore.

Surface Bactericidal Activity Assay: The Japanese Industrial Standard test for surface microbicidal activity (JIS Z 2801:2000[43]) was used to evaluate the bactericidal activity of dropcast coated glass coverslips in duplo with each three replicates (Figure S2A, Supporting Information). Prior to the experiment, the dropcast films were sterilized for 15 min with UV-C. In short, bacteria were cultured in TSB to the logarithmic growth phase at 37 °C and 130 rpm. Subsequently, the bacteria were washed in PBS and diluted with RPMI to 5.5×10^5 CFU mL^{-1}, based on the OD_{620}. 30 µL of the diluted bacterial culture, containing $\approx 1.65 \times 10^4$ CFU, was pipetted on the surface of each sample and parafilm (Ø 12 mm) was carefully placed on top. After overnight incubation at 37 °C in a humid atmosphere, each sample was placed in 2 mL of PBS containing 0.025% SPS, vortexed for 15 s, sonicated for 10 min in a sonicator water bath (Elma Transsonic T460, 35 kHz; Elma) and vortexed for 30 s to dislodge adherent bacteria. This procedure does not affect bacterial viability.[53] Per sample, two independent tenfold serial dilutions were made in a microtiter plate and duplicate 10 µL aliquots of the undiluted suspension and of the dilutions were pipetted onto blood agar plates. To further increase the detection limit, the remaining liquid was centrifuged at maximum speed for 2 min and the pellet was resuspended in 100 µL PBS and plated on blood agar plates. The blood agar plates were incubated overnight at 37 °C and the numbers of colonies were counted the following day.

In the optimization experiments, performed to establish the method of seeding for the in vivo studies, the JIS test as described above was performed with the following modifications (Figure S2B, Supporting Information). Two times 6.25 µL of an inoculum of *S. aureus* JAR060131 in water was applied at dipcoated glass coverslips (Ø 8 mm) and air-dried for ≈10 min. Samples were either sonicated directly after drying to perform a quantitative culture or left for overnight incubation. For the latter, two droplets of 6.25 µL PBS were added on top of the inoculated sample, covered with parafilm (Ø 4 mm), incubated overnight and quantitatively cultured as described above. In the experiments, various inocula of 6.9×10^5, 2.6×10^6, 1.6×10^6, 6.8×10^5, 8.5×10^4 CFU per material were used.

To evaluate the bactericidal activity of the dipcoated titanium implants against *S. aureus* JAR060131 before implantation in the mouse, the JIS test as described above was performed with the following modifications (Figure S2B, Supporting Information). Two times 6.25 µL of an inoculum of 3.2×10^7 CFU mL^{-1} *S. aureus* JAR060131 in water was applied at both sides of the implant (total of 4×10^5 CFU in 12.5 µL) and air-dried for ≈10 min. Subsequently, two droplets of 6.25 µL PBS were added on top of the inoculated sample, covered with parafilm (Ø 4 mm), incubated overnight and quantitatively cultured as described above.

Cell Culture with (UPy-)SAAP-148GG Additives in Solution: NHDFs (Lonza) were cultured in Dulbecco's modified Eagle medium (DMEM) with high glucose and pyruvate (Thermo Fisher Scientific), supplemented with 1% v/v penicillin and streptomycin (Life Technologies) and 1% v/v glutaMAX (Gibco) under standard culturing conditions at 37 °C and 5% CO_2. A 96-flatbottom well plate (Greiner Bio) was used for the experiment and the cells were seeded at a density of 7500 cells per cm^2. After 1 day, the culture medium was removed, and fresh culture medium supplemented

with SAAP-148 or UPy-C_6-SAAP-148 or UPy-C_{12}-SAAP-148, with a concentration range of 0–240 × 10^{-6} M, was added to the cells.

The mitochondrial activity was determined after 24 h of culture. After 24 h, the culture medium was removed, and the samples were washed with PBS. Culture medium enriched with 44 × 10^{-6} M of Resazurin was incubated on the samples at 37 °C for 3 h. Per sample, 2 aliquots of 100 µL resazurin-enriched medium were transferred to a black 96-well plate (Greiner) and fluorescence was measured (ex = 550 nm, em = 584 nm) with a Synergy HT plate reader and Gen5 software (BioTek Instruments, Inc.). Resulting fluorescence was corrected for background fluorescence. Experiments were performed with five replicates per condition.

Cell Culture on Dropcast Polymer Films: NHDFs were cultured in DMEM with high glucose and pyruvate, supplemented with 1% v/v penicillin and streptomycin and 1% v/v glutaMAX under standard culturing conditions at 37 °C and 5% CO_2. Both experiments with and without 10% v/v FBS (Lonza) supplemented in the media were performed. PCLdiUPy films were dropcast on 14 mm Ø glass coverslips as described before. To prevent film detachment from the glass coverslips, custom holders were used during cell culture. Each holder consisted of a 12-well Transwell insert (Corning) without a membrane and a ring which clicked on the insert and fixated the polymer films on top of the glass coverslips. The used insert system constricted the cells to adhere to the films on the glass coverslips. The constructs were subjected to UV-C sterilization for 20 min and washed with PBS, afterward cells were seeded at a density of 15 600 cells cm^{-2} on the polymer films. During the experiment, two different medium compositions were studied, 1) complete culture medium with 10% FBS and 2) complete culture medium without FBS.

The mitochondrial activity and adhering cell number were determined after 24 h of culture. After 24 h, for the mitochondrial activity, the culture medium was removed, and the samples were washed with PBS. Culture medium enriched with 44 × 10^{-6} M of Resazurin was incubated on the samples at 37 °C for 3 h. Per sample, 2 aliquots of 200 µL resazurin-enriched medium were transferred to a black 96-well plate (Greiner) and fluorescence was measured (ex = 550 nm, em = 584 nm) with a Synergy HT plate reader and Gen5 software (BioTek Instruments, Inc.). Resulting fluorescence was corrected for background fluorescence and normalized to PCLdiUPy. Experiments were performed with six replicates per condition.

For the adhering cell number, the culture medium was removed after 24 h of culture and the cells were gently washed three times with PBS and fixated with 3.7% v/v formaldehyde solution (Merck) + 0.5% v/v Triton X-100 v/v (Merck) in PBS at room temperature (RT) for 15 min. All washing steps were performed in triplo. The samples were washed with PBS and stained for the actin cytoskeleton with phalloidin-Atto 488 (dilution 1:300) in 0.05% Triton X-100 v/v in PBS at RT for 45 min. Thereafter, the samples were washed and stained for the nucleus via incubation with 4′-6 diamidino-2-phenylindole (0.1 μg mL^{-1}) for 10 min. Finally, the samples were washed again with PBS and mounted with mowiol. Images were acquired in a pre-determined pattern which covered three images per sample to estimate cell distribution over the whole sample. This experiment was performed with three replicates per condition. Nuclei were counted with the help of ImageJ 1.53c (National Institutes of Health, USA). Images were acquired with use of a Leica SP8 confocal microscope and LAS x software (Leica) for samples cultured with FBS and a Zeiss Axiovert 200M and Axiovision software (Zeiss) for samples cultured without FBS.

Mouse Subcutaneous BAI Model: The mouse study was approved by the Animal Welfare Body of the Amsterdam UMC (location AMC), Amsterdam, The Netherlands (study number: 19-8484-1-03). Specific pathogen-free C57BL/6J OlaHsd immune competent female mice (Envigo RMS B.V., The Netherlands) aged ≈8 to 10 weeks and weighing 17 to 20 g were used. Mice were housed individually for the short duration of the experiment in individually ventilated cages and were provided with sterile food and water ad libitum. Groups of nine mice with either two uncoated, PCLdiUPy-coated, or 5 mol% UPy-SAAP-148GG-coated titanium implants each (n = 18 implants per group) were used in the experiments. Prior to implantation, the uncoated titanium implants and PCLdiUPy-coated implants (i.e., 0 mol% UPy-SAAP-148GG) were sterilized with EtO, while implants coated with 5 mol% UPy-SAAP-148GG were sterilized with 15 min UV-C exposure. Per time point, mice were randomized over the experimental groups using an online random sequence generator. The investigators were blinded for the group allocation during the experiment and processing of the outcome.

The subcutaneous BAI experiment was performed in a mouse model as described previously.[9] Briefly, the mice received a subcutaneous injection of buprenorphine (Temgesic, RB Pharmaceuticals Limited; 0.05 mg kg^{-1}) 30 min prior to the start of the experiment for pain control. Subsequently, the mice were anaesthetized with 2% isoflurane (Pharmachemie) in oxygen in a laminar flow cabinet, followed by shaving the back of the mice using an electric razor and disinfecting the area with 70% ethanol. On each side, an incision of 0.4 cm was made 1 cm lateral to the spine. Immediately before implantation, the surface of the (coated) titanium implants was pre-inoculated with two times 6.25 µL (total of 4 × 10^5 CFU in 12.5 µL) of a 3.2 × 10^7 CFU mL^{-1} *S. aureus* JAR060131 inoculum and air-dried for ≈10 min in a laminar flow cabinet. Subsequently, the (coated) implants were implanted subcutaneously with minimal tissue damage using a transponder. The incisions were closed with a single 0/6 vicryl stitch.

At 1 or 4 days after implantation, mice were anesthetized with isoflurane in oxygen and Temgesic was administered 30 min before explanation for pain control. Standardized biopsies (Ø 12 mm) were taken from the implantation sites.[36] Each biopsy included skin, subcutaneous tissue, and the implant. The implants were separated from the tissue and both the implant and tissue were cut in two equal halves. One half was used for quantitative culture of bacteria, the other half was stored for optional future analyses. The implants were vortexed briefly in 0.5 mL of PBS to remove nonadherent bacteria, and then sonicated in fresh PBS for 5 min in a water bath sonicator to dislodge all bacteria. The tissue samples were homogenized in 0.5 mL of PBS containing 0.025% SPS using five zirconia beads (Ø 2 mm, BioSpec Products) and the MagnaLyser System (Roche), with three cycles of 30 s at 7000 rpm, with 30 s cooling on ice between cycles. The sonicates and homogenates were tenfold serially diluted and 50 µL was plated on agar. The numbers of cultured bacteria were expressed as log CFU per sample. The lower limit of detection was 10 CFU. To visualize the data on a logarithmic scale, a value of 1 CFU was assigned when no growth occurred.

Statistical Analysis: All statistical analyses were performed with Graphpad Prism. The in vivo data were analyzed with two-sample comparisons using a Kruskal–Wallis test followed by a Mann–Whitney rank sum test. The significance of differences between the frequencies of categorical variables was determined using Fisher's exact test, and between percentages with analysis of variance. For all tests, p-values of ≤0.05 were considered significant.

Schematic figures were created with BioRender.com

Supporting Information

Supporting Information is available from the Wiley Online Library or from the author.

Acknowledgements

M.G.J.S. and M.R., and S.A.J.Z. and P.Y.W.D. contributed equally to this work. The authors thank Ardine de Vos and Karen Schröder-Bonneveld (Animal Research Institute AMC (ARIA), Amsterdam UMC) and Clara Guarch-Pérez (Dept. of Medical Microbiology and Infection Prevention, Amsterdam UMC) for their excellent support in the animal experiments. Dr. Jan-Wouter Drijfhout (Dept. of Immunohematology and Blood Transfusion, Leiden University Medical Centre) is acknowledged for his advice on the peptide synthesis and providing SAAP-148. This research was financially supported by the DPI, project no. 731.015.505, the Ministry of Education, Culture and Science (Gravity Programs 024.001.035 and 024.003.013), and the research program of Chemelot InSciTe, project EyeSciTe.

Conflict of Interest

The authors declare no conflict of interest.

Data Availability Statement

The data that support the findings of this study are available from the corresponding author upon reasonable request.

Keywords

antimicrobial peptides, biomaterial-associated infections, coatings, SAAP-148, supramolecular biomaterials, titanium, ureido-pyrimidinone

Received: November 1, 2022
Revised: April 3, 2023
Published online: May 28, 2023

[1] H. Chouirfa, H. Bouloussa, V. Migonney, C. Falentin-Daudré, *Acta Biomater.* **2019**, *83*, 37.
[2] E. J. Tobin, *Adv. Drug Delivery Rev.* **2017**, *112*, 88.
[3] G. Radley, I. L. Pieper, C. A. Thornton, *J. Biomed. Mater. Res., Part B* **2018**, *106*, 1730.
[4] S. D. Elek, P. E. Conen, *Br. J. Exp. Pathol.* **1957**, *38*, 573.
[5] W. Zimmerli, C. Moser, *FEMS Immunol. Med. Microbiol.* **2012**, *65*, 158.
[6] C. A. N. Broekhuizen, M. J. Schultz, A. C. van der Wal, L. Boszhard, L. de Boer, C. M. J. E. Vandenbroucke-Grauls, S. A. J. Zaat, *Crit. Care Med.* **2008**, *36*, 2395.
[7] B. A. S. Knobben, Y. Engelsma, D. Neut, H. C. van der Mei, H. J. Busscher, J. R. van Horn, *Clin. Orthop. Relat. Res.* **2006**, *452*, 236.
[8] C. R. Arciola, D. Campoccia, L. Montanaro, *Nat. Rev. Microbiol.* **2018**, *16*, 397.
[9] M. Riool, L. De Boer, V. Jaspers, C. M. Van Der Loos, W. J. B. Van Wamel, G. Wu, P. H. S. Kwakman, S. A. J. Zaat, *Acta Biomater.* **2014**, *10*, 5202.
[10] N. Kavanagh, E. J. Ryan, A. Widaa, G. Sexton, J. Fennell, S. O'rourke, K. C. Cahill, C. J. Kearney, F. J. O'brien, S. W. Kerrigan, *Clin. Microbiol. Rev.* **2018**, *31*, e00084.
[11] W. Zimmerli, A. Trampuz, *Implant-Associated Infection*, Springer, New York **2011**.
[12] E. A. Masters, R. P. Trombetta, K. L. De Mesy Bentley, B. F. Boyce, A. L. Gill, S. R. Gill, K. Nishitani, M. Ishikawa, Y. Morita, H. Ito, S. N. Bello-Irizarry, M. Ninomiya, J. D. Brodell, C. C. Lee, S. P. Hao, I. Oh, C. Xie, H. A. Awad, J. L. Daiss, J. R. Owen, S. L. Kates, E. M. Schwarz, G. Muthukrishnan, *Bone Res.* **2019**, *7*, 20.
[13] S. Zaat, C. Broekhuizen, M. Riool, *Future Microbiol.* **2010**, *5*, 1149.
[14] G. J. A. ter Boo, D. W. Grijpma, T. F. Moriarty, R. G. Richards, D. Eglin, *Biomaterials* **2015**, *52*, 113.
[15] M. Morgenstern, A. Vallejo, M. A. McNally, T. F. Moriarty, J. Y. Ferguson, S. Nijs, W. Metsemakers, *Bone Joint Res.* **2018**, *7*, 447.
[16] H. Turgut, S. Sacar, I. Kaleli, M. Sacar, I. Goksin, S. Toprak, A. Asan, N. Cevahir, K. Tekin, A. Baltalarli, *BMC Infect. Dis.* **2005**, *5*, 91.
[17] M. Riool, A. de Breij, J. W. Drijfhout, P. H. Nibbering, S. A. J. Zaat, *Front. Chem.* **2017**, *5*, 63.
[18] H. J. Busscher, H. C. van der Mei, G. Subbiahdoss, P. C. Jutte, J. J. A M van den Dungen, S. A. J. Zaat, M. J. Schultz, D. W. Grainger, *Sci. Transl. Med.* **2012**, *4*, 153rv10.
[19] S. Qin, K. Xu, B. Nie, F. Ji, H. Zhang, *J. Biomed. Mater. Res., Part A* **2018**, *106*, 2531.
[20] K. E. Greber, M. Dawgul, *Curr. Top. Med. Chem.* **2016**, *17*, 620.
[21] C. de la Fuente-Núñez, M. H. Cardoso, E. de Souza Cândido, O. L. Franco, R. E. W. Hancock, *Biochim. Biophys. Acta, Biomembr.* **2016**, *1858*, 1061.
[22] L. Yu, K. Li, J. Zhang, H. Jin, A. Saleem, Q. Song, Q. Jia, P. Li, *ACS Appl. Bio Mater.* **2022**, *5*, 366.
[23] F. Costa, I. F. Carvalho, R. C. Montelaro, P. Gomes, M. C. L. Martins, *Acta Biomater.* **2011**, *7*, 1431.
[24] M. J. Webber, E. A. Appel, E. W. Meijer, R. Langer, *Nat. Mater.* **2015**, *15*, 13.
[25] R. P. Sijbesma, F. H. Beijer, L. Brunsveld, B. J. B. Folmer, J. H. K. K. Hirschberg, R. F. M. Lange, J. K. L. Lowe, E. W. Meijer, *Science* **1997**, *278*, 1601.
[26] F. H. Beijer, R. P. Sijbesma, H. Kooijman, A. L. Spek, E. W. Meijer, *J. Am. Chem. Soc.* **1998**, *120*, 6761.
[27] E. Wisse, A. J. H. Spiering, P. Y. W. Dankers, B. Mezari, P. C. M. M. Magusin, E. W. Meijer, *J. Polym. Sci., Part A: Polym. Chem.* **2011**, *49*, 1764.
[28] H. Kautz, D. J. M. Van Beek, R. P. Sijbesma, E. W. Meijer, *Macromolecules* **2006**, *39*, 4265.
[29] B. J. B. Folmer, R. P. Sijbesma, R. M. Versteegen, J. A. J. van der Rijt, E. W. Meijer, *Adv. Mater.* **2000**, *12*, 874.
[30] P. Y. W. Dankers, M. C. Harmsen, L. A. Brouwer, M. J. A. Van Luyn, E. W. Meijer, *Nat. Mater.* **2005**, *4*, 568.
[31] S. H. M. Söntjens, R. A. E. Renken, G. M. L. Van Gemert, T. A. P. Engels, A. W. Bosman, H. M. Janssen, L. E. Govaert, F. P. T. Baaijens, *Macromolecules* **2008**, *41*, 5703.
[32] S. Spaans, P.-P. K. H. Fransen, M. J. G. Schotman, R. van der Wulp, R. P. M. Lafleur, S. G. J. M. Kluijtmans, P. Y. W. Dankers, *Biomacromolecules* **2019**, *20*, 2360.
[33] S. Zaccaria, R. C. Van Gaal, M. Riool, S. A. J. Zaat, P. Y. W. Dankers, *J. Polym. Sci., Part A: Polym. Chem.* **2018**, *56*, 1926.
[34] G. Wang, J. L. Narayana, B. Mishra, Y. Zhang, F. Wang, C. Wang, D. Zarena, T. Lushnikova, X. Wang, *Design of Antimicrobial Peptides: Progress Made with Human Cathelicidin LL-37*, Vol. *1117*, Springer, Singapore **2019**.
[35] M. J. Nell, G. S. Tjabringa, A. R. Wafelman, R. Verrijk, P. S. Hiemstra, J. W. Drijfhout, J. J. Grote, *Peptides* **2006**, *27*, 649.
[36] A. De Breij, M. Riool, P. H. S. Kwakman, L. De Boer, R. A. Cordfunke, J. W. Drijfhout, O. Cohen, N. Emanuel, S. A. J. Zaat, P. H. Nibbering, T. F. Moriarty, *J. Controlled Release* **2016**, *222*, 1.
[37] A. de Breij, M. Riool, R. A. Cordfunke, N. Malanovic, L. de Boer, R. I. Koning, E. Ravensbergen, M. Franken, T. van der Heijde, B. K. Boekema, P. H. S. Kwakman, N. Kamp, A. El Ghalbzouri, K. Lohner, S. A. J. Zaat, J. W. Drijfhout, P. H. Nibbering, *Sci. Transl. Med.* **2018**, *10*, eaan4044.
[38] T. A. E. Ahmed, R. Hammami, *J. Food Biochem.* **2019**, *43*, e12546.
[39] Y. Liang, X. Zhang, Y. Yuan, Y. Bao, M. Xiong, *Biomater. Sci.* **2020**, *8*, 6858.
[40] E. M. Haisma, A. de Breij, H. Chan, J. T. van Dissel, J. W. Drijfhout, P. S. Hiemstra, A. El Ghalbzouri, P. H. Nibbering, *Antimicrob. Agents Chemother.* **2014**, *58*, 4411.
[41] N. Al Naiemi, B. Duim, P. H. M. Savelkoul, L. Spanjaard, E. de Jonge, A. Bart, C. M. Vandenbroucke-Grauls, M. D. de Jong, *J. Clin. Microbiol.* **2005**, *43*, 4862.
[42] W. P. J. Appel, G. Portale, E. Wisse, P. Y. W. Dankers, E. W. Meijer, *Macromolecules* **2011**, *44*, 6776.
[43] Japanese Standards Association, *Japanese Industrial Standards*, Japanese Standards Association, Japan **2000**.
[44] B. D. Ippel, B. Arts, H. M. Keizer, P. Y. W. Dankers, *J. Polym. Sci., Part B: Polym. Phys.* **2019**, *57*, 1725.
[45] B. B. Mollet, M. Comellas-Aragonès, A. J. H. Spiering, S. H. M. Söntjens, E. W. Meijer, P. Y. W. Dankers, *J. Mater. Chem. B* **2014**, *2*, 2483.

[46] G. S. Dijksteel, M. M. W. Ulrich, P. H. Nibbering, R. A. Cordfunke, J. W. Drijfhout, E. Middelkoop, B. K. H. L. Boekema, *J. Microbiol. Antimicrob.* **2020**, *12*, 70.
[47] T. F. Moriarty, D. Campoccia, S. K. Nees, L. P. Boure, R. G. Richards, *Int. J. Artif. Organs* **2010**, *33*, 667.
[48] D. Campoccia, L. Montanaro, T. F. Moriarty, R. G. Richards, S. Ravaioli, C. R. Arciola, *Int. J. Artif. Organs* **2008**, *31*, 841.
[49] K. Nishitani, W. Sutipornpalangkul, K. L. De Mesy Bentley, J. J. Varrone, S. N. Bello-Irizarry, H. Ito, S. Matsuda, S. L. Kates, J. L. Daiss, E. M. Schwarz, *J. Orthop. Res.* **2015**, *33*, 1311.
[50] H. G. Windmueller, C. J. Ackerman, R. W. Engel, *J. Biol. Chem.* **1959**, *234*, 895.
[51] L. Chen, C. Sloey, Z. Zhang, P. V. Bondarenko, H. Kim, D. Ren, S. Kanapuram, *J. Pharm. Sci.* **2015**, *104*, 731.
[52] M. G. M. C. Mori da Cunha, B. Arts, L. Hympanova, R. Rynkevic, K. Mackova, A. W. Bosman, P. Y. W. Dankers, J. Deprest, *Acta Biomater.* **2020**, *106*, 82.
[53] J. J. Boelens, J. Dankert, J. L. Murk, J. J. Weening, T. van der Poll, K. P. Dingemans, L. Koole, J. D. Laman, S. A. J. Zaat, *J. Infect. Dis.* **2000**, *181*, 1337.
[54] J. J. Boelens, S. A. J. Zaat, J. Meeldijk, J. Dankert, *J. Biomed. Mater. Res.* **2000**, *50*, 546.
[55] C. A. N. Broekhuizen, L. de Boer, K. Schipper, C. D. Jones, S. Quadir, R. G. Feldman, J. Dankert, C. M. J. E. Vandenbroucke-Grauls, J. J. Weening, S. A. J. Zaat, *Infect. Immun.* **2007**, *75*, 1129.
[56] C. A. N. Broekhuizen, L. de Boer, K. Schipper, C. D. Jones, S. Quadir, C. M. J. E. Vandenbroucke-Grauls, S. A. J. Zaat, *J. Biomed. Mater. Res., Part A* **2008**, *85A*, 498.
[57] C. A. N. Broekhuizen, M. Sta, C. M. J. E. Vandenbroucke-Grauls, S. A. J. Zaat, *Infect. Immun.* **2010**, *78*, 954.
[58] Z. Li, D. Lee, X. Sheng, R. E. Cohen, M. F. Rubner, *Langmuir* **2006**, *22*, 9820.
[59] A. Stepulane, A. K. Rajasekharan, M. Andersson, *ACS Appl. Bio Mater.* **2022**, *5*, 5289.
[60] Y. Li, R. Chen, F. Wang, X. Cai, Y. Wang, *RSC Adv.* **2022**, *12*, 6918.
[61] I. De Feijter, O. J. G. M. Goor, S. I. S. Hendrikse, M. Comellas-Aragonès, S. H. M. Söntjens, S. Zaccaria, P. P. K. H. Fransen, J. W. Peeters, L.-G. Milroy, P. Y. W. Dankers, N. Nh, **2015**, *26*, 2707.
[62] P. H. S. Kwakman, A. A. te Velde, L. de Boer, D. Speijer, C. M. J. E. Vandenbroucke-Grauls, S. A. J. Zaat, *FASEB J.* **2010**, *24*, 2576.
[63] Z. Oren, J. Ramesh, D. Avrahami, N. Suryaprakash, Y. Shai, R. Jelinek, *Eur. J. Biochem.* **2002**, *269*, 3869.
[64] L. E. R. O'Leary, J. A. Fallas, E. L. Bakota, M. K. Kang, J. D. Hartgerink, *Nat. Chem.* **2011**, *3*, 821.